

Experimental measurements of the flow resistance and inductance of inertance tubes at high acoustic amplitudes

Y.L. Ju ^{*}, G.Q. He, Y.K. Hou, J.T. Liang, Y. Zhou

Cryogenic Laboratory, Technical Institute of Physics and Chemistry, Chinese Academy of Sciences, P.O. Box 2711, Beijing 100080, China

Received 15 March 2002; accepted 21 June 2002

Abstract

We measured the flow resistance and flow inductance of inertance tubes at high acoustic amplitudes for four different inner diameters of 0.6, 1.0, 1.5 and 2.0 mm at various tube length ranging from 100 to 1500 mm, at frequencies of 30, 40, 50, 60 and 70 Hz. The experiments were carried out under system mean pressure of 20 bar at room temperature. The experimental data were compared with the explicit solution to the linear momentum equation for small acoustic amplitudes and were fitted with the modification coefficients in terms of the operating frequency and Reynolds numbers characterized by the amplitude of gas velocities.

© 2002 Elsevier Science Ltd. All rights reserved.

Keywords: Experimental measurements; Oscillating flow; Inertance tube

1. Introduction

Compared with Stirling coolers, pulse tube coolers have a considerable advantage due to no mechanical moving parts at low temperatures. This leads to much more reliable operation and longer life times for low-temperature components and considerable low mechanical vibrations and electromagnetic interference from the cooler itself. However, the Stirling cooler has demonstrated better thermal efficiency than the pulse tube cooler because the low-temperature displacer of such cooler can be driven at a phase that is adjusted to give the best cooling performance although the efficiency of the pulse tube cooler has been improved greatly with the introduction of orifice and buffer by Mikulin et al. [1] and double-inlet by Zhu et al. [2]. Most of this due to the absence of solid displacer in the pulse tube, the phase shifter located at room temperature does not lead to an efficient phase shift of the high density working gas in the low-temperature region [3,4].

In 1994 Kanao et al. [5] found improved performance in their 50 Hz pulse tube cooler when they replaced the orifice with a long capillary tube (neck tube). Later,

Godshalk et al. [6] used inertial effects in the pulse tube in a 350 Hz orifice pulse tube cooler to make the cooler performance better. Recent studies [7] described a simple way of an inertance tube, to replace the orifice, at the warm end of the pulse tube to generate a proper phase shift to improve the performance of pulse tube coolers. The inertance tube is a long, thin tube that provides a complex impedance at the warm end of the pulse tube rather than a simple resistive impedance provided by the orifice. The inertance tube adds a reactive impedance, analogous to inductance in a simple AC electrical circuit, that allows the phase difference between the pressure and mass flow rate in the pulse tube to be adjusted to an extent as efficiently as Stirling coolers. In brief, the inertance tube is an acoustic term connecting both inertia resistance and inductance of moving gas [7].

Many investigations showed that use of the inertance tube is significantly beneficial for large-scale pulse tubes or at higher operating frequencies [8,9]. They indicate that the improvement in the performance by using the inertance tube comes from: (1) it can produce a desirable phase shift between the pressure and mass flow in the pulse tube, (2) it can balance the intrinsic tendency for DC gas flow in the double-inlet pulse tube cooler; and (3) it can increase work flow per mass flow within the pulse tube.

However, little information is available on experimental measurements of the flow resistance and flow

^{*} Corresponding author. Tel.: +86-10-62627302; fax: +86-10-62564049.

E-mail address: yonglin@cl.cryo.ac.cn (Y.L. Ju).

conductance of the inertance tube, particularly, at high acoustic amplitudes. In this work, experiments were performed to measure the flow resistance and flow inductance of inertance tubes at high acoustic amplitudes. We firstly gave a brief mathematical formulation for the flow resistance and flow inductance of the inertance tube at low acoustic amplitudes and the explicit solution to the linear momentum equation were presented. Then we measured the flow resistance and flow inductance of inertance tubes at high acoustic amplitudes for four different inner diameters of 0.6, 1.0, 1.5 and 2.0 mm at various tube length ranging from 100 to 1500 mm, at frequencies of 40, 50, 60 and 70 Hz. The experiments were carried out under system mean pressure of 20 bar at room temperature. The results were compared with the explicit solution at small acoustic amplitudes and were fitted with the modification coefficients in terms of the operating frequency and Reynolds numbers characterized by the amplitude of velocities.

2. Analysis

To simplify the analysis and to avoid the complicated mathematics as much as possible, we restrict our attention to an incompressible flow oscillating sinusoidally in an inertance tube of inner radius $r = a$, and of length L connecting two large reservoirs at room temperatures $T = T_0$. The outer sidewall of the tube is thermally insulating (adiabatic). The tube is filled with pressurized helium gas (we restrict attention to ideal gases), which moves back and forth with the oscillatory pressure p at the angular frequency $\omega = 2\pi f$. We assume the maximum Reynolds number associated with the oscillation is not too high (laminar flow) and one can neglect end effects. Gas velocity u is in the x -direction only and varies only in the r -coordinate direction normal to the tube wall. Within these limitations, the momentum equation becomes

$$\rho \frac{\partial u}{\partial t} + u \frac{\partial u}{\partial x} = -\frac{\partial p}{\partial x} + \mu \frac{1}{r} \frac{\partial}{\partial r} \left(r \frac{\partial u}{\partial r} \right) \quad (1)$$

Here μ is the dynamic viscosity. The nonlinear inertia term $u(\partial u/\partial x)$ in Eq. (1) can be neglected at low acoustic amplitudes

$$\rho \frac{\partial u}{\partial t} = -\frac{\partial p}{\partial x} + \mu \frac{1}{r} \frac{\partial}{\partial r} \left(r \frac{\partial u}{\partial r} \right) \quad (2)$$

One can easily derive that the gas velocity of the one-dimensional flow in the tube is in the form

$$u_0 = \frac{1}{\rho_0 \omega} \frac{\partial p_0}{\partial x} \left[1 - \frac{J_0(\sqrt{2}r/\delta_v)}{J_0(\sqrt{2}a/\delta_v)} \right] \quad (3)$$

where u_0 and p_0 are the amplitude of the gas velocity and pressure oscillation, respectively, J_0 is the Bessel func-

tion of the first kind of order zero, and $\delta_v = \sqrt{2\mu/\rho_0\omega}$ is the viscous penetration depth denoting the relevant boundary-layer thickness [10]. Upon integrating and averaging Eq. (3) over the cross-sectional area $S = \pi a^2$ one yields the cross-sectional mean velocity in the tube

$$\bar{u}_0 = \frac{1}{2a} \int_{-a}^a u_0 dr = \frac{1}{\rho_0 \omega} \frac{\partial p_0}{\partial x} \left[1 - \frac{2J_1(Ka)}{KaJ_0(Ka)} \right] \quad (4)$$

Here we introduce a parameter $K = \sqrt{2}/\delta_v$. As we know the term $-\partial p_0/\partial x$ is the pressure drop per unit tube length and $-S\partial p_0/\partial x$ is the force on the tube per unit length, thereby the force impedance per unit tube length can be expressed as

$$Z'_M = -S \frac{\partial p_0}{\partial x} / \bar{u}_0. \quad (5)$$

Substituting Eq. (4) into Eq. (5), we have

$$Z'_M = -\frac{\rho_0 \omega S}{1 - (2J_1(Ka))/(KaJ_0(Ka))} \quad (6)$$

Integrating Eq. (6) over the total length L of the tube and assuming L is much smaller than the local sound wavelength, we find the force impedance along the total tube

$$Z_M = \int_0^L Z'_M dx = -\frac{\rho_0 \omega SL}{1 - (2J_1(Ka))/(KaJ_0(Ka))} \quad (7)$$

The flow impedance is defined as

$$Z_A = Z_M/S^2 \quad (8)$$

Thus

$$Z_A = -\frac{\rho_0 \omega L/S}{1 - (2J_1(Ka))/(KaJ_0(Ka))} \quad (9)$$

The flow impedance Z_A is complex in general and can be simply approximated as

$$Z_A = \frac{8\mu L}{\pi a^4} \sqrt{1 + |Ka|^2/32} + j \frac{\rho_0 \omega L}{\pi a^2} \left(1 + \frac{1}{\sqrt{32 + |Ka|^2/2}} \right) \quad (10)$$

Its real part and imaginary part indicates the flow resistance and flow inductance, respectively,

$$R_A = \frac{8\mu L}{\pi a^4} \sqrt{1 + |Ka|^2/32} \quad (11)$$

$$X_A = \frac{\rho_0 \omega L}{\pi a^2} \left(1 + \frac{1}{\sqrt{32 + |Ka|^2/2}} \right) \quad (12)$$

The correlation equation of the flow resistance coefficient (friction factor) is usually given by

$$f = \frac{\Delta p}{\rho \bar{u}_0^2/2} \frac{D}{L} \quad (13)$$

It can be rewritten as

$$f = \frac{2D^2/L}{\mu Re_0} \frac{\Delta p}{\bar{u}_0} \quad (14)$$

here $Re_0 = \rho \bar{u}_0 D / \mu$ is the Reynolds number based on the cross-sectional mean velocity. According to Eqs. (5)–(8) we have the flow resistance

$$R_A = S \frac{\Delta p}{\bar{u}_0 S^2} \quad (15)$$

Combining with Eq. (14), one yields

$$f = \frac{2D^2/L}{\mu Re_0} R_A S \quad (16)$$

Substituting Eq. (11) into Eq. (16) we find the flow resistance coefficient f for the inertance tube under oscillatory flow conditions

$$f = \frac{64}{Re_0} \sqrt{1 + \frac{|Ka|^2}{32}} \quad (17)$$

It is well known that the flow factor of the tube for the steady-state flow is given as follows

$$f_{st} = \frac{64}{Re_0} \quad (18)$$

Comparing Eq. (17) to Eq. (18) one yields

$$\beta = \frac{f}{f_{st}} = \sqrt{1 + \frac{|Ka|^2}{32}} > 1 \quad (19)$$

It is worth noting that Eq. (17) is obtained based on two assumptions: (1) at low acoustic amplitudes, and (2) the length of the tube is much smaller than the local sound wavelength of the working gas. Eq. (19) indicates that at low acoustic amplitudes the flow resistance coefficient of the inertance tube in the oscillatory flow is larger by a factor of β than that of a steady-state flow at the same Reynolds numbers.

Fig. 1 shows the factor of β of inertance tubes with diameters of 0.6, 1.0, 1.5 and 2.0 mm as a function of frequency. It shows that the factor of β is in the range of 1.04–1.1 for 0.6 mm tube, and of 1.4–1.8 for 2 mm tube, respectively.

However, the correlation given above based on the assumption of the low acoustic amplitudes is usually not applicable for a pulse tube cooler operating at high acoustic amplitudes (large pressure amplitudes), in which the nonlinear inertia term $u(\partial u / \partial x)$ in Eq. (1) cannot be neglected. Therefore, we introduce here two modification coefficients C_1 and C_2 for considering the nonlinear effects at high acoustic amplitudes.

$$R'_A = C_1 R_A \quad (20)$$

$$X'_A = C_2 X_A \quad (21)$$

In the next section we will describe the experimental procedures for R'_A and X'_A measurements to determine the modification coefficients of C_1 and C_2 .

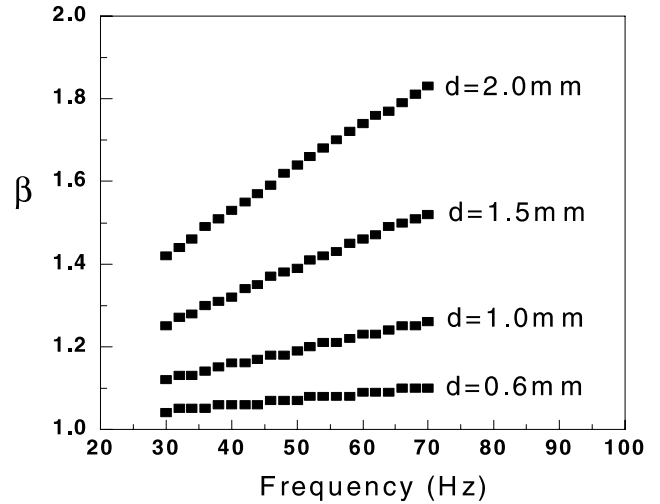


Fig. 1. The factor of β as a function of frequency for different inertance tube diameters.

3. Experiments

The schematic of the experimental set-up to determine the value of C_1 and C_2 is shown in Fig. 2, which is similar as shown in Ref. [11], except the main test section. Therefore, only a streamlined summary of experimental technique is described here. The oscillatory flow is generated by means of a self-made linear compressor. The swept volume of the compressor is around 2 cm³, and its working frequency can be adjustable from 20 to 80 Hz. The test section of different inertance tubes is made of thin wall stainless steel tube. At one end of the test section is placed a flow straightener (a short tube of 8.9 mm in inner diameter and 65 mm in length with 10 mm filled with 100 mesh cooper screens). A reservoir (volume of 74.5 cm³) is directly connected to the other end of the test section.

We have employed two small quartz differential pressure transducers (KISTLER, Type 601A), connected to charge amplifiers (KISTLER, Type 5011) to measure transient pressure oscillations at the inlet of the inertance tube, and inside the reservoir. The transducer

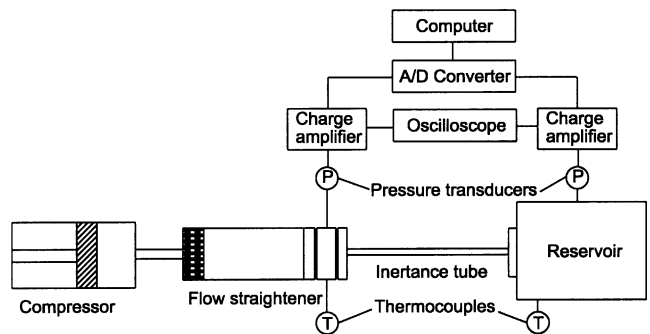


Fig. 2. Schematic diagram of experimental apparatus.

has a high natural frequency of 150 kHz. As the typical frequencies of a pulse tube cooler are much smaller than the natural frequency, we can safely ignore the error in measuring the amplitude and phase delay of the pressure oscillations. Two thermocouples are placed on the surface of the flow straightener and in the reservoir to measure the temperatures. Analog-to-digital conversions are carried out by an A/D conversion board (KEITHLEY, DAS 1610), which is plugged into a personal computer. An oscilloscope (HP 5402B) is also employed to simultaneously observe the pressure wave signals.

The cross-sectional mean velocity of the oscillatory flow is determined by measuring the instantaneous pressure oscillations in the reservoir. Since this approach has already been described in the literatures [12,13], we show the results without describing the details. Since the transient pressure oscillation p_{res} in the reservoir in a pulse tube cooler has usually a small pressure amplitude, it is reasonable to assume $p_{\text{res}} = p_0 + p_1 e^{j\omega t}$, with p_0 and $p_1 e^{j\omega t}$ are the steady and oscillatory part of the pressure in the reservoir, respectively. The relationship between the gas mass and the pressure in the reservoir is approximated as

$$\frac{dm}{dt} = \frac{V_{\text{res}}}{\gamma R T_{\text{res}}} \frac{dp_{\text{res}}}{dt} \quad (22)$$

where γ is the ratio of isobaric to isochoric specific heats and R ideal gas constant. The subscript ‘res’ denotes variables in the reservoir and V_{res} is the volume of the reservoir. Both the pressure ratio and the amplitude of the temperature are small in the reservoir, so that the gas temperature T_{res} in the reservoir can be regarded as the room temperature. The mass flux entering or leaving the reservoir is

$$\frac{d\dot{m}}{dt} = \rho \bar{u} A_t = \frac{V_{\text{res}}}{c^2} \frac{dp_{\text{res}}}{dt} \quad (23)$$

where A_t is the cross-sectional area of the flow straightener connecting to the reservoir and $c = \sqrt{\gamma R T}$ is the local sound speed. With $dp_{\text{res}} = dp_1 e^{j\omega t}$ the amplitude of the gas velocity at the inlet of the reservoir can be simply expressed as

$$\bar{u} = \frac{p_1 V_{\text{res}} \omega}{A_t \rho c^2} e^{j(\omega t + \frac{\pi}{2})} \quad (24)$$

By measuring the transient pressure oscillations in the reservoir and using Eq. (24) one can determine the cross-sectional mean velocity of the oscillatory gas flow. We have used hot wire anemometer to measure the velocity of the oscillatory flow [11]. The average relative derivation between the velocities obtained by the hot wire anemometer and evaluated by Eq. (24) is about 3.35%, which is within experimental error.

Strictly speaking, Eq. (24) is valid only at (1) the volume of the inertance tube is much smaller than the

volume of the reservoir, and (2) the tube length L is much smaller than the local sound wavelength of the working gas.

4. Results and discussion

In this section we shall present experimental results for R'_A and X'_A measurements to determine the modification coefficients C_1 and C_2 . Experiments were carried out for four different inner diameters (0.6, 1.0, 1.5 and 2.0 mm) at various tube length ranging from 100 to 1500 mm, at frequencies of 30, 40, 50, 60 and 70 Hz. The working gas was helium and the system mean pressure was 2.0 MPa at room temperature. In order to determine the pressure amplitudes and their phase angle, the raw experimental data measured from the pressure transducers need data processing. The output signal of the pressure transducer was first amplified, pressure transformation and correction, and then collected with the spectrum analysis for high frequency harmonic filtration and Fourier analysis.

Fig. 3 illustrates the typical variation of the transient pressure waves at inlet of the inertance tube and in the reservoir. Fig. 3(a) is the raw experimental data measured from the pressure transducer. It shows that the pressure waves are, strictly, not sinusoidal oscillations and they include high-order frequency terms besides fundamental frequency. Fig. 3(b) and (c) are the spectrum analyses of the raw experimental data of pressure oscillations at inlet of the inertance tube and in the reservoir, respectively. It shows clearly that the intensities of the higher-order frequencies are much smaller than that of the fundamental frequency. Fig. 3(d) is the pressure wave after the high-order frequency harmonic filtration. It clearly demonstrates the amplitude and the phase angle of the pressure wave. The average uncertainty in the pressure amplitude and phase angle was evaluated to be less than 2%.

After obtained the transient pressures of p_t and p_{res} at the inlet of the inertance tube and in the reservoir and the amplitude of the gas velocity by using Eq. (24), we can further calculate the flow impedance by using

$$Z_A = (p_t - p_{\text{res}}) / A_t \bar{u} = R'_A + jX'_A \quad (25)$$

Together with Eqs. (20) and (21) we can determine the modification coefficients of C_1 and C_2 in terms of Re_0 and f .

A series of experiments have been carried out to determine the modification coefficients C_1 and C_2 . Experimental results demonstrated that the flow resistance and inductance of inertance tubes at higher acoustic amplitudes strongly depend on the operating frequency and Reynolds numbers based on the amplitude of the

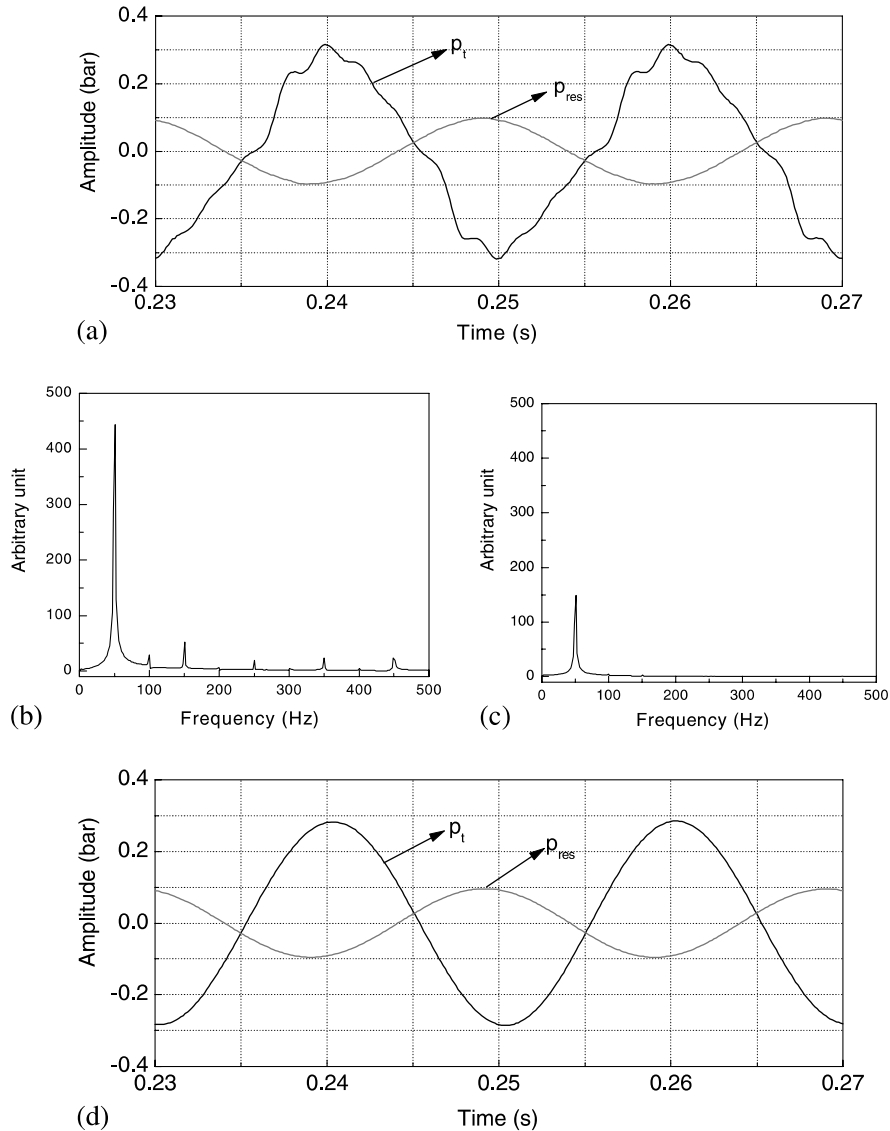


Fig. 3. A typical variation of dynamic pressures and its filter wave ($\varnothing 2 \text{ mm} \times 1.5 \text{ mm}$): (a) raw data; (b) spectrum analysis of p_1 ; (c) spectrum analysis of p_{res} ; (d) filter wave.

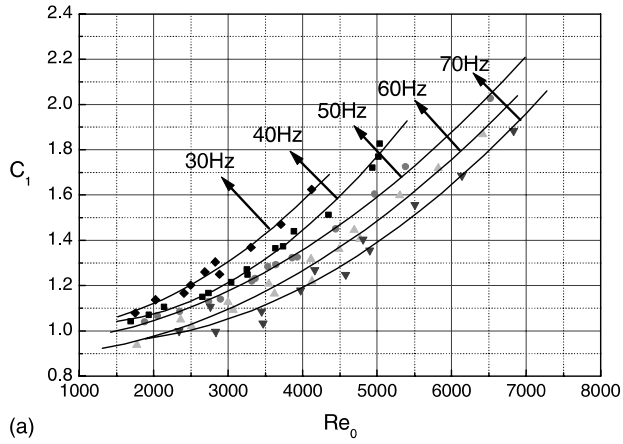
cross-sectional mean velocity. The selected experimental results are summarized in Figs. 4–6.

Fig. 4(a–c) show the experimental data of the correlation coefficient C_1 of the flow resistance of inertance tubes for three different tube diameters of 0.6, 1.0 and 2 mm, respectively, in terms of Re_0 and f . We find that the modification coefficient C_1 of the flow resistance (pure flow resistance) varies with different tube diameters, but is nearly independent of the length of the inertance tube. It is shown clearly that the correlation coefficient C_1 increases monotonically with increasing Reynolds numbers and with decreasing operating frequencies. It means that the nonlinear effect becomes larger with the increasing of the amplitude of velocities. The correlation coefficient C_1 gradually tends to 1 when the Reynolds numbers reach to zero. Therefore, the explicit solution of Eq. (11) for

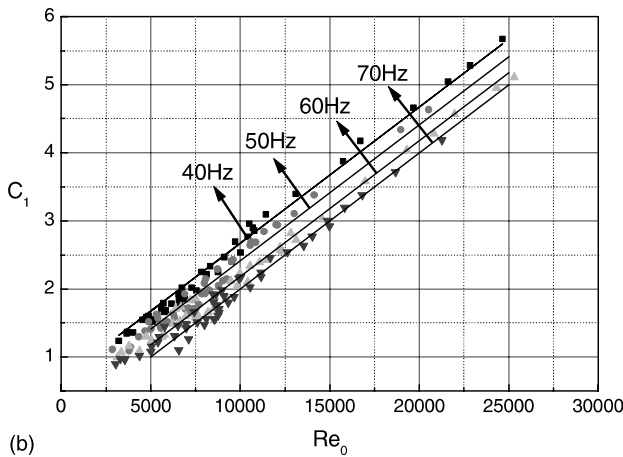
small acoustic amplitudes is only applicable to small Reynolds numbers.

A comparison of the correlation coefficient C_1 for different tube diameters at the same Reynolds numbers shows that the larger the tube diameter, the smaller the C_1 . The reason is obvious: the velocity is small for large inner diameter tube at the same Reynolds numbers thereby the nonlinear effects become relatively weak.

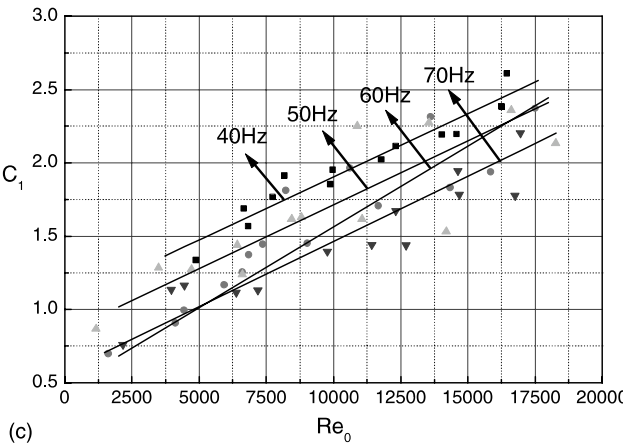
For the inertance tube of 0.6 mm inner diameter, the experimental data are well fitted by the correlation equation of second-order polynomial of $C_1 = A_0 + A_1 Re + A_2 Re^2$ (here A_0 , A_1 , and A_2 are fitted constant varied with operating frequency). While for the inertance tube with inertance tubes of 1.0, 1.5 and 2 mm, the experimental data are well fitted by the correlation equation of first-order polynomial of $C_1 = B_0 + B_1 Re$



(a)



(b)

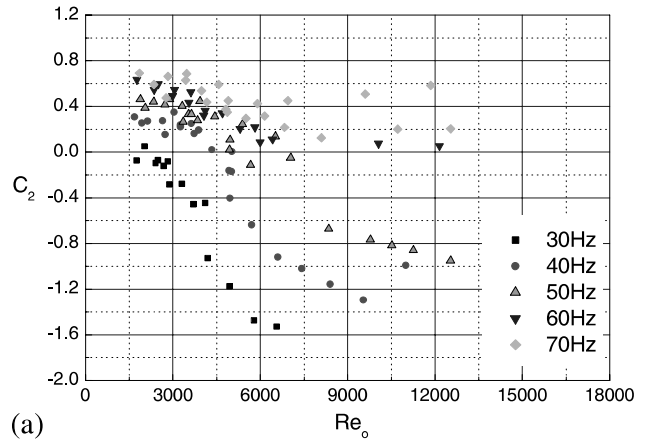


(c)

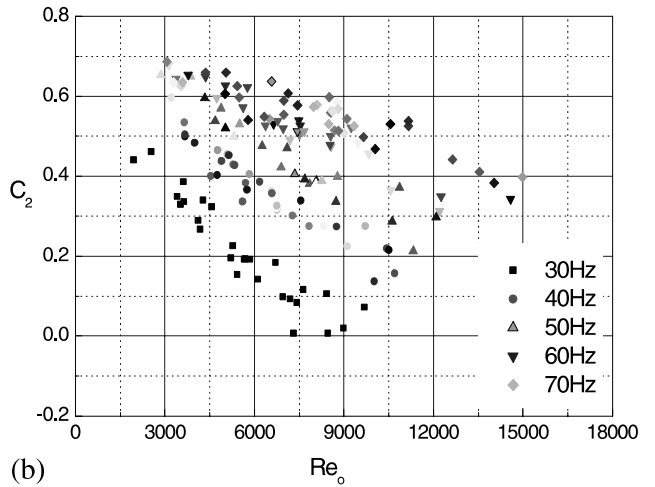
Fig. 4. The correlation coefficient C_1 in terms of Reynolds numbers and frequency for different diameters of inertance tubes: (a) 0.6; (b) 1.0; (c) 2.0 mm.

(here B_0 and B_1 are fitted constant varied with operating frequency).

Fig. 5(a) and (b) present the experimental data of the modification coefficient C_2 of the flow inductance of inertance tubes for two different tube diameters of 0.6 and 1.0 mm, respectively, in terms of Re_0 and f . It is shown that the correlation coefficients of C_2 are less than



(a)



(b)

Fig. 5. The correlation coefficient C_2 in terms of Reynolds numbers and frequency for different diameters of inertance tubes: (a) 0.6 and (b) 1.0 mm.

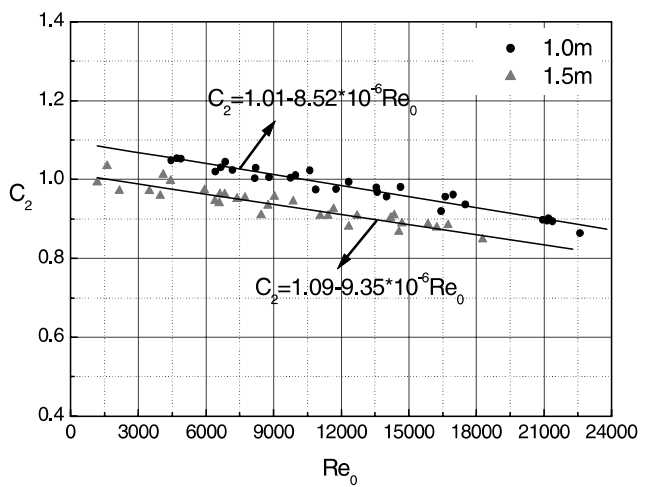


Fig. 6. The correlation coefficient C_2 in terms of Reynolds numbers for different length of inertance tubes.

1, which means that the flow inductance of the inertance tube at high acoustic amplitudes is smaller than

that at low acoustic amplitudes. The C_2 decreases with increasing Reynolds numbers, and increases with increasing operating frequencies, which is contrary to the tendency of the correlation coefficient C_1 of the flow resistance. However, the influence of the operating frequency on the correlation coefficient C_2 gradually becomes smaller with the increasing of the tube diameter. We also find that the correlation coefficients of C_2 for the inertance tube with inner diameters of 0.6 and 1.0 mm are nearly independent of the length of the inertance tube, similar as that of C_1 . Whereas, for the inertance tube with 2.0 mm inner diameter, C_2 is almost independent of the operating frequency, but slightly depends on the length of the inertance tube, as shown in Fig. 6.

In conclusion, we have measured the flow resistance and flow inductance of inertance tubes at high acoustic amplitudes for four different inner diameters (0.6, 1.0, 1.5 and 2.0 mm) at various tube length ranging from 100 to 1500 mm, at frequencies of 30, 40, 50, 60 and 70 Hz. The experimental data were compared with the explicit solution to the linear momentum equation for small acoustic amplitudes and were fitted with the modification coefficients in terms of the operating frequency and Reynolds numbers characterized by the amplitude of gas velocities.

From these experimental results we can see evidently the difference of the flow resistance and flow inductance of inertance tubes at high and low acoustic amplitudes. It is helpful for understanding the physical mechanism of the inertance tube subjected to the oscillating gas flow in high frequency pulse tube operations and further conduct theoretical analysis.

Acknowledgements

The work is funded by the National Natural Science Foundation of China (grant no. 50176052).

References

- [1] Mikulin EI, Tarasov AA, Shrebyonock MP. Low-temperature expansion pulse tube. *Adv Cry Eng* 1984;29:629.
- [2] Zhu S, Wu P, Chen Z. Double inlet pulse tube refrigerator—an important improvement. *Cryogenics* 1990;30:514.
- [3] Ju YL, Wang C, Zhou Y. Dynamic experimental investigation of a multi-bypass pulse tube refrigerator. *Cryogenics* 1997;37:357.
- [4] Ju YL. Computational study of a 4 K two-stage pulse tube cooler with mixed Eulerian–Lagrangian method. *Cryogenics* 2001;41:49.
- [5] Kanao K, Watanabe N, Kanazawa Y. A miniature pulse tube refrigerator for the temperature below 100 K. *Cryogenics* 1994; 34:167.
- [6] Godshalk KM, Jin C, et al. Characterization of 350 Hz thermoacoustic driven orifice pulse tube refrigerator with measurements of the phase of the mass flow and pressure. *Adv Cry Eng* 1996;41:1411.
- [7] Gardner DL, Swift GW. Use of inertance in orifice pulse tube refrigerators. *Cryogenics* 1997;37:117.
- [8] Wang C, Thummes G, Heiden C. Control of DC gas flow in a single-stage pulse tube cooler. *Cryogenics* 1998;38:843.
- [9] Kotsubo V, Huang P, Nast TC. Observation of DC flows in a double inlet pulse tube. *Cryocoolers* 1999;10:299.
- [10] Swift GW. Thermoacoustic engines. *J Acoust Soc Am* 1988; 84:1145.
- [11] Ju YL, Jiang Y, Zhou Y. Experimental study of the oscillating flow characteristics for regenerator in pulse tube cryocooler. *Cryogenics* 1998;38:649.
- [12] Nishitani T, Nakano K, Maruno Y, Yanai M. Investigation of acoustic streaming and steady flow in the orifice of single stage pulse tube refrigerator, JSJS-5, Osaka, Japan, p. 66.
- [13] Lu GQ, Cheng P. Flow characteristics of a metering valve in a pulse tube refrigerator. *Cryogenics* 2000;40:721.